



HHS Public Access

Author manuscript

Cell Rep. Author manuscript; available in PMC 2021 December 17.

Published in final edited form as:

Cell Rep. 2021 May 11; 35(6): 109125. doi:10.1016/j.celrep.2021.109125.

A high-throughput genome-wide RNAi screen identifies modifiers of survival motor neuron protein

Nikki M. McCormack¹, Mahlet B. Abera¹, Eveline S. Arnold², Rebecca M. Gibbs², Scott E. Martin³, Eugen Buehler³, Yu-Chi Chen³, Lu Chen³, Kenneth H. Fischbeck², Barrington G. Burnett^{1,4,*}

¹Department of Anatomy, Physiology and Genetics, Uniformed Services University of the Health Sciences, F. Edward Hébert School of Medicine, Bethesda, MD 20814, USA

²Neurogenetics Branch, National Institute of Neurological Disorders and Stroke, Bethesda, MD 20892, USA

³Functional Genomics Lab, National Center for Advancing Translational Sciences, National Institutes of Health, Bethesda, MD 20850, USA

⁴Lead contact

SUMMARY

Spinal muscular atrophy (SMA) is a debilitating neurological disorder marked by degeneration of spinal motor neurons and muscle atrophy. SMA results from mutations in *survival motor neuron 1 (SMN1)*, leading to deficiency of survival motor neuron (SMN) protein. Current therapies increase SMN protein and improve patient survival but have variable improvements in motor function, making it necessary to identify complementary strategies to further improve disease outcomes. Here, we perform a genome-wide RNAi screen using a luciferase-based activity reporter and identify genes involved in regulating SMN gene expression, RNA processing, and protein stability. We show that reduced expression of Transcription Export complex components increases SMN levels through the regulation of nuclear/cytoplasmic RNA transport. We also show that the E3 ligase, Neurl2, works cooperatively with Mib1 to ubiquitinate and promote SMN degradation. Together, our screen uncovers pathways through which SMN expression is regulated, potentially revealing additional strategies to treat SMA.

Graphical Abstract

This is an open access article under the CC BY-NC-ND license (<http://creativecommons.org/licenses/by-nc-nd/4.0/>).

*Correspondence: barrington.burnett@usuhs.edu.

AUTHOR CONTRIBUTIONS

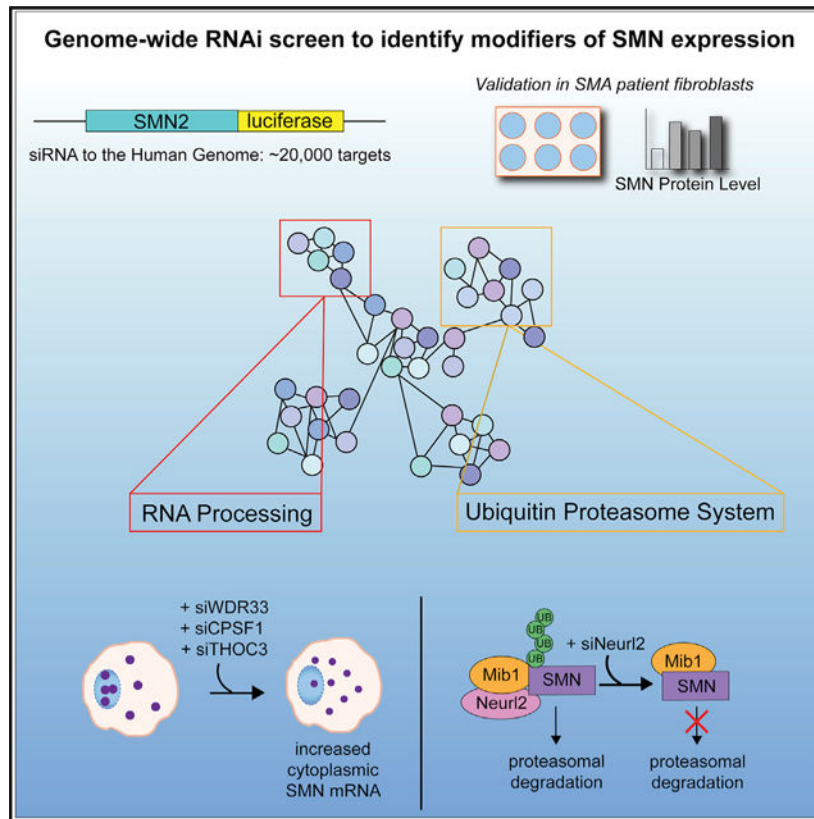
N.M.M., M.B.A., E.S.A., R.M.G., S.E.M., E.B., Y.-C.C., L.C., K.H.F., and B.G.B. designed and performed experiments and analyzed the data. N.M.M., K.H.F., and B.G.B. contributed to the writing of the manuscript. All authors discussed the results and conclusions and reviewed the manuscript.

DECLARATION OF INTERESTS

The authors declare no competing interests.

SUPPLEMENTAL INFORMATION

Supplemental information can be found online at <https://doi.org/10.1016/j.celrep.2021.109125>.



In brief

Treatments for spinal muscular atrophy aim to increase survival motor neuron (SMN) protein. Using a genome-wide RNAi screen, McCormack et al. identify modifiers of SMN expression, including genes that are involved in transcription regulation, RNA processing, and protein stability.

INTRODUCTION

Spinal muscular atrophy (SMA) is a neuromuscular disease that is one of the leading genetic causes of infant mortality (Lefebvre et al., 1995). SMA is characterized by the loss of lower motor neurons in the anterior horn of the spinal cord and muscle atrophy leading to muscle weakness (Lefebvre et al., 1995). SMA is caused by the homozygous loss of *survival motor neuron 1 (SMN1)*, the predominant producer of survival motor neuron (SMN) protein (Lefebvre et al., 1995; Lorson et al., 1999). Humans have a second copy of this gene, *SMN2*, which has a cytosine-to-thymine base pair change leading to exclusion of exon 7 in the transcript to primarily produce a truncated form of SMN known as SMN 7 (Lorson et al., 1999; Monani et al., 1999a). *SMN2* is unable to fully compensate for the loss of *SMN1* in patients with SMA leading to a deficiency of SMN protein. Patients with SMA have variable copy numbers of *SMN2*, which correlates with disease severity (Mailman et al., 2002; Wirth et al., 2006). Although the critical function of SMN in the context of SMA is not completely known, SMN has been shown to be required for the assembly of small

nuclear ribonucleoproteins (snRNPs) (Pellizzoni et al., 2002). It remains unclear how loss of SMN contributes to SMA pathology.

Restoration of SMN protein has been shown to ameliorate the disease phenotype. Strategies to increase SMN in SMA animal models and patients include increasing *SMN2* transcription, promoting exon 7 inclusion, blocking SMN protein degradation, and gene delivery (Abera et al., 2016; Avila et al., 2007; Hua et al., 2008; Passini et al., 2010). Currently, there are three recently approved treatments for patients with SMA: nusinersen, an antisense oligonucleotide, which increases SMN protein levels by promoting the inclusion of exon 7 in the *SMN2* transcript; gene therapy (Zolgensma), which uses an adeno-associated virus (AAV)-9 to deliver *SMN1* complementary DNA (cDNA) to patients; and risdiplam, a small molecule that corrects *SMN2* splicing (Foust et al., 2010; Hua et al., 2008; Mendell et al., 2017; Poirier et al., 2018). Although some patients have significant improvements in their ability to sit, walk, and run, other patients see little to no improvement in their motor function (Aragon-Gawinska et al., 2020; Finkel et al., 2017; Mendell et al., 2017; Mercuri et al., 2018). For example, in one study, only 32% of SMA type 1 patients were able to sit unassisted for 30 s following 14 months of nusinersen treatment (Aragon-Gawinska et al., 2020). Therefore, ongoing clinical trials and research focus on identifying alternative ways to further increase SMN protein levels or complementary strategies to improve disease outcomes by targeting non-SMN-modifying genes and pathways.

In addition to *SMN2*, only two disease modifiers have been identified: plastin-3 and neurocalcin delta (Oprea et al., 2008; Riessland et al., 2017). Plastin-3 is upregulated in unaffected *SMN1*-deleted females (Oprea et al., 2008). Expression of neurocalcin delta is reduced in asymptomatic, *SMN1*-deleted individuals with four copies of *SMN2* (Riessland et al., 2017). Upregulation of plastin-3, an actin-binding protein, lessens disease severity potentially by stabilizing the growth cone, while downregulation of neurocalcin delta alleviates the disease phenotype by restoring endocytosis in SMA mice (Kaifer et al., 2017; Oprea et al., 2008; Riessland et al., 2017). To date, very few regulators of SMN transcript have been reported. Histone deacetylase (HDAC) inhibitors have been used in cell and animal models of the disease to increase SMN transcript levels (Avila et al., 2007; Sumner et al., 2003) but have been shown to have limited efficacy in clinical trials (Kissel et al., 2011, 2014; Swoboda et al., 2010). Moreover, HDAC inhibitors have been reported to activate expression of ~2% of the genome, which reduces enthusiasm to further develop these drugs for SMA treatment (Kelly et al., 2002; Pazin and Kadonaga, 1997; Van Lint et al., 1996).

Given that current treatment modalities increase SMN levels, it is important to determine all the factors that regulate SMN protein expression. In this study, we sought to identify, using an unbiased approach, modifiers of SMN protein levels utilizing a genome-wide cell-based RNAi screen against >20,000 individual genes. Human embryonic kidney 293 (HEK293) cells stably expressing an *SMN2* luciferase minigene cassette were used as the cellular model system for the screen, and subsequent validation analyses were carried out using SMA patient-derived fibroblasts. We have identified and validated regulators of SMN expression that were grouped into transcriptional regulation, RNA processing, and protein stability.

RESULTS

Genome-wide RNAi screen identifies genes that regulate SMN expression

To identify modifiers of SMN expression, we conducted a genome-wide RNAi screen using HEK293 cells that stably express an *SMN2* luciferase minigene (Zhang et al., 2001). The luciferase reporter gene assay combines the promoter and splicing-based cassettes in tandem with the major portion of the native *SMN2* cDNA with luciferase (Figure 1A). Luciferase is expressed when full-length SMN protein is generated with luminescence signal proportional to SMN protein levels. The screen was conducted in two stages (Figure 1A). To determine baseline signals, standard deviation values, and optimal incubation times post-transfection, we conducted an initial screen using the Ambion Silencer Select Version 4 Human Druggable Genome comprising a non-pooled library of three independent small interfering RNAs (siRNAs) targeting 10,415 genes that are predicted to be druggable. Primary screening data have been deposited into PubChem under the assay ID 1347426. The initial screen was completed successfully with robust *SMN2* luciferase expression that could be detected following siRNA transfection. Several genes when knocked down altered luciferase expression, including genes that were previously shown to modulate SMN protein expression (shown in italics) (Table S1) (Hastings et al., 2007; Kashima et al., 2007a; Wee et al., 2014). We next performed a follow-up genome-wide RNAi screen (Figure 1A) using the Ambion genome-wide siRNA library, which is composed of three independent siRNAs targeting 21,556 genes. Candidate gene selection used a robust statistical measure of median absolute deviation (MAD) to standardize siRNA activities from each screen (Chung et al., 2008). Common seed analysis was used to help prioritize clean hits as opposed to those appearing to arise from seed-based off-target effects (Buehler et al., 2012; Marine et al., 2012). Outcomes of screened siRNAs with a positive *Z* score reflect enhanced full-length SMN expression and a negative *Z* score showing a reduction in SMN levels (Figure 1B). To identify strong modifiers, we set a *Z* score cutoff of greater than 1.0 or less than -1.0 (2-fold change). *Z* score analyses indicated a continuous distribution of hits (Figure 1B); 112 genes gave *Z* scores smaller than -1.0 (reduced expression) and 89 larger than +1.0 (increased expression), ranging from -5.5 to +3.3 (Tables S2 and S3). Several previously described regulators of SMN expression were re-identified in the screen (Figure S1), thus validating the effectiveness of our assay.

We divided hits into groups based on predicted molecular functions to gain better insight into pathways that would lead to enhancement of SMN protein levels. We found an enrichment of genes involved in RNA processing and protein metabolism (Figure 1C). Additionally, we sorted the top 100 hits by protein class using Protein Annotation Through Evolutionary Relationship (PANTHER) analysis and found several genes that encode for nucleic acid binding proteins and protein-modifying enzymes (Table 1).

Identification of SMN exon 7 splicing regulators

An overwhelming number of genes (75 out of 201 hits) had well-characterized roles in mRNA splicing, indicating that splicing alterations might be the most robust mechanism to increase SMN expression. Of the SMN-modifying genes, we identified several genes that have previously been shown to enhance SMN exon 7 inclusion. The previously described

SMN2 splicing modifiers hnRNP A1, hnRNP A2, U2AF1, U2AF2, PUF60, and SRSF3 were all high-scoring hits in the screen (Table 2) (Hastings et al., 2007; Kashima et al., 2007a; Martins de Araújo et al., 2009; Wee et al., 2014). All these genes were previously shown to promote SMN exon 7 exclusion consistent with an increase in full-length SMN expression when they were inactivated. Interestingly, genes previously described to promote SMN inclusion (ASF/SF2 [SRSF1], SRp30c, Tra2- β , TIA1) were not picked up in the screen (Cartegni and Krainer, 2002; Hofmann et al., 2000; Singh et al., 2011; Young et al., 2002). This may point to the limitations of this assay to detect genes that further suppress SMN expression, as well as genes that have redundant roles in regulating SMN expression.

Gene cluster and interactome analyses

We next sought to determine whether specific cellular pathways altered SMN expression by grouping hits into functional clusters using Search Tool for the Retrieval of Interacting Genes/Proteins (STRING) analysis (Szklarczyk et al., 2017). The 201 genes that met our initial selection criteria (increased or decreased SMN expression) were selected for further analysis (Figure 2A). We looked for over-representation of biological functions among the candidate genes by gene set enrichment analysis using the Kyoto Encyclopedia of Genes and Genomes (KEGG), Reactome, Gene Ontology (GO), and PANTHER databases.

Key components of the RNA polymerase II transcription machinery, including the mediator complex, were highly enriched in the genes that when knocked down reduced SMN expression, consistent with their role as transcriptional activators. Indeed, knockdown of CDK8, Med6, Med8, Med14, Med17, Med20, Med24, Med26, Med27, Med30, or Med31 all resulted in decreased SMN expression (Figure 2B). Using STRING analysis, we identified two distinct network clusters that regulated SMN expression: the Transcription-Export (TREX) complex and the ubiquitin-proteasome system (Figure 2B).

The TREX complex regulates SMN levels

Although *SMN2* splicing has been well studied, little is known about the factors that regulate SMN mRNA nucleocytoplasmic trafficking. The TREX complex couples transcription elongation by RNA polymerase II to mRNA export (Katahira, 2012). TREX coordinates with the elongating RNA polymerase II and facilitates RNP assembly and recruitment of RNA processing factors. Depletion of TREX components reduces expression of some, but not all, genes (Mason and Struhl, 2005). We found from our screen that siRNA targeting *THOC1*, *THOC4* (*ALYREF*), *NFX1*, and *CPSF6* reduced SMN expression, suggesting they may be indispensable to SMN mRNA nucleocytoplasmic translocation.

Interestingly, we found that knocking down *THOC3*, another member of the TREX complex, increased SMN expression. This result seemingly conflicts with its predicted role in nuclear export of mRNA (Katahira, 2012). It has been proposed that the TREX and cleavage and polyadenylation specificity factor (CPSF) complexes play sequential roles in mRNA maturation and trafficking (Chan et al., 2011; Katahira, 2012). Unlike other TREX complex subunits, *THOC3* contains a WD40 repeat domain, like the CPSF complex protein WDR33, suggesting that both proteins may have redundant or complementary roles in

mRNA processing (Chan et al., 2011; Heath et al., 2016). We selected CPSF1, THOC3, and WDR33 to further investigate their roles in SMN RNA processing.

We transfected cells with siRNA targeting *CPSF1*, *WDR33*, and *THOC3* and isolated protein and mRNA 48 h after transfection. We confirmed that knocking down each gene individually (*WDR33* mRNA: 84% decrease, $p < 0.0001$; *CPSF1* mRNA: 87% decrease, $p < 0.0001$; *THOC3* mRNA: 89% decrease, $p < 0.0001$) increased SMN protein levels (si*WDR33*: 70% increase, $p = 0.0064$; si*CPSF1*: 71% increase, $p = 0.0043$; si*THOC3*: 75% increase, $p = 0.0205$) (Figures 3A and 3B). Additionally, simultaneously transfecting SMA patient-derived fibroblasts with all three siRNAs significantly increased SMN protein levels over control (171% increase; $p = 0.0418$) (Figures 3C and 3D). Knockdown of the three genes together resulted in a similar increase in SMN as each of the individual knockdowns (Figure S2). We next examined whether knocking down each gene altered *SMN2* transcription, mRNA stability, or cytoplasmic translocation. To determine whether knocking down each gene affected *SMN2* transcription, we used RT-PCR primers spanning SMN intron-exon boundaries to quantify *SMN2* precursor mRNA (pre-mRNA). We found that *SMN2* pre-mRNA levels were not changed by knocking down *CPSF1* ($p = 0.5059$) or *THOC3* ($p = 0.9635$) but are significantly increased when *WDR33* is knocked down (51% increase; $p = 0.0131$) (Figure 4A). In addition, total *SMN2* mRNA was unchanged by knocking down each gene ($p = 0.5643$) (Figure 4B). We next examined whether knocking down *CPSF1*, *WDR33*, and *THOC3* affects *SMN2* mRNA stability. We treated SMA patient cells with actinomycin D to stop gene transcription and collected cells at the designated time points. We found no difference in the rate of degradation of the *SMN2* mRNA when *CPSF1*, *WDR33*, or *THOC3* was knocked down (Figure 4C). To investigate whether knockdown of either *CPSF1*, *WDR33*, and *THOC3* affected *SMN2* splicing, we collected cell pellets from SMA patient-derived fibroblasts 48 h after transfection with siRNA targeting *CPSF1*, *WDR33*, and *THOC3*; isolated RNA; and converted mRNA to cDNA. *SMN2* cDNA was amplified by PCR and resolved by agarose gel electrophoresis. We found that the ratio of full-length SMN to SMN 7 was not altered when either *CPSF1* ($p = 0.0537$), *WDR33* ($p = 0.8984$), or *THOC3* ($p = 0.9990$) was knocked down (Figure 4D).

Lastly, we looked at the nucleocytoplasmic distribution of *SMN2* mRNA after knocking down each gene. Purity of nuclear and cytoplasmic fractions was verified by examining mRNA levels of MALAT1 and ACTB (Figure S3). Nuclear *SMN2* mRNA was reduced following knockdown of *WDR33* ($p = 0.0040$), *CPSF1* ($p = 0.0014$), and *THOC3* ($p = 0.0014$), whereas we found increased cytoplasmic localization of the *SMN2* mRNA 48 h after knocking down *WDR33* ($p < 0.0001$), *CPSF1* ($p < 0.0001$), and *THOC3* ($p = 0.0001$), offering one explanation for increased SMN expression (Figure 4E). Together, we show that components of the mRNA trafficking complexes are enriched in our screen and confirm in patient cells that knocking down *CPSF1*, *WDR33*, and *THOC3* increases SMN expression. Knockdown of *WDR33* slightly increased *SMN2* pre-mRNA levels, but total *SMN2* mRNA levels remained unchanged. Although we found no evidence that each gene altered *SMN2* mRNA stability or splicing, knocking down *WDR33*, *CPSF1*, and *THOC3* increased the cytoplasmic abundance of *SMN2* mRNA.

Reducing expression of core components of the ubiquitin-proteasome system increases SMN levels

Functional clustering analysis revealed enrichment of genes regulating SMN expression, including those involved in protein clearance. We and others have shown that SMN protein stability is regulated by the ubiquitin-proteasome pathway (Burnett et al., 2009; Chang et al., 2004; Gray et al., 2018; Han et al., 2012; Hsu et al., 2010; Kwon et al., 2013; Locatelli et al., 2015; Powis et al., 2016). From the screen, we identified core components of the ubiquitin-proteasome degradation system that when knocked down increase SMN levels (Figure 2B). These genes include *UBA1*, the enzyme that catalyzes the first step in the ubiquitin conjugation cascade, which is responsible for tagging proteins for trafficking and degradation (Amm et al., 2014). Interestingly, mutations in *UBA1* have been previously associated with X-linked infantile SMA (Ramser et al., 2008), and increasing *UBA1* expression improves the disease phenotype in SMA mice (Powis et al., 2016).

We have shown that the E3 ubiquitin ligase mindbomb-1 (Mib1) directly ubiquitinates and promotes the degradation of SMN (Kwon et al., 2013). Here, we found siRNAs that target the E2-conjugating enzyme *UBE2D3*, which works in combination with Mib1 to ubiquitinate target proteins, also increase SMN protein levels (Figure 2B). We confirmed in patient-derived cells that knocking down *UBE2D3* increases SMN levels (Figure S1B). Although E1 and E2 activating and conjugating enzymes drive the initial stages of protein ubiquitination, the E3 ligase is responsible for the substrate specificity for protein ubiquitination. In addition to Mib1, the screen re-identified the E3 ligase UCHL1 (Figure S1B), which has previously been confirmed to regulate SMN protein levels (Hsu et al., 2010), and two additional E3 ligases, SIAH1 and neuralized-2 (*Neur12*), as potential regulators of SMN levels. We confirmed in SMA patient-derived fibroblasts that knocking down *Neur12*, but not *SIAH1*, increased SMN levels (80% increase, $p < 0.0001$) (Figure 5A). Altogether, we confirmed here that the ubiquitin-proteasome system is a major regulator of SMN protein levels and identified additional genes that may contribute to regulating SMN protein stability, either together or independently.

Neur12 interacts with SMN and regulates its turnover

We next sought to determine whether *Neur12* regulated SMN expression through direct association and ubiquitination. SMA patient fibroblasts were transfected with GFP-*Neur12* or *Neur12*-GFP, and endogenous SMN was immunoprecipitated followed by western blot analysis with an anti-GFP antibody. We found robust association of *Neur12* and SMN, confirming interaction (Figure 5B). We next examined the potential mechanism through which *Neur12* affected SMN protein stability. We investigated if, like Mib1, *Neur12* ubiquitinates SMN. We transfected SMA patient-derived fibroblasts with hemagglutinin (HA)-tagged *Neur12* and collected lysates 48 h after transfection. We immunoprecipitated SMN from these lysates and quantified SMN ubiquitination by western blot analysis. We found that overexpressing *Neur12* and Mib1 individually increased SMN ubiquitination (*Neur12*: 89% increase, $p = 0.0305$; Mib1: 320% increase, $p < 0.0001$) (Figure 5C). Interestingly, knocking down *Neur12* prevented Mib1-dependent SMN ubiquitination (Mib1 versus Mib1 + si*Neur12*: 46% decrease in ubiquitination, $p < 0.0001$). Co-transfecting siRNA to *Neur12* with an siRNA-resistant *Neur12* (*Neur12_{res}*) restored Mib1-dependent

SMN ubiquitination, confirming that *Neurl2*, and not off-target effects of the siRNA, modulates SMN ubiquitination (*Mib1* versus *Mib1* + si*Neurl2* + *Neurl2*_{res}; $p = 0.7566$) (Figure 5C). To determine whether *Neurl2* directly ubiquitinates SMN, we performed an *in vitro* ubiquitination assay. Because we did not know which E2-conjugating enzyme would facilitate *Neurl2*-dependent SMN ubiquitination, we performed the assay in the presence of each known E2-conjugating enzyme. We found that *Neurl2* directly ubiquitinates SMN only in the presence of the E2 enzyme *Ubch1* (Figure 5D). *Neurl2* has been reported to, in cooperation with *Mib1*, ubiquitinate and decrease expression of X-Delta (Song et al., 2006). Therefore, we asked whether *Mib1* and *Neurl2* cooperatively modulated SMN levels. Knocking down *Mib1* and *Neurl2* separately increases SMN levels in SMA patient cells (si*Neurl2*: 73% increase, $p = 0.0060$; si*Mib1*: 81% increase, $p = 0.0027$). Knocking down *Mib1* and *Neurl2* together resulted in similar increases in SMN levels (81% increase compared with control) as knocking down each ligase individually, suggesting both enzymes function together or in series (si*Neurl2* versus si*Neurl2* + si*Mib1*: $p = 0.9740$; si*Mib1* versus si*Neurl2* + si*Mib1*: $p > 0.9999$) (Figure 5E). Finally, we investigated whether *Neurl2* cooperates with *Mib1* to regulate the rate of SMN turnover. We compared the rate of SMN turnover in cells transiently overexpressing *Mib1*, alone or when *Neurl2* is knocked down. Consistent with our previous studies, SMN is more rapidly degraded in cells overexpressing *Mib1* (Figure 5F). However, the rate of SMN turnover is slowed when *Neurl2* levels are reduced, suggesting that both genes cooperate to regulate SMN turnover (control versus si*Neurl2* 8 h: $p = 0.0447$; 16 h: $p = 0.0036$).

DISCUSSION

The recently approved therapies to treat SMA have dramatically improved survival and reduced motor deficits of patients with the most severe form of SMA. However, many patients with SMA remain severely debilitated, suggesting additional treatments to improve or complement the current therapies are sorely needed. Based on the current SMA landscape, several SMN-dependent and -independent therapeutic strategies are under clinical consideration, including efforts to provide systemic boosting of SMN levels or enhance skeletal muscle size and function. In this study, we opted to utilize a human genome-wide RNAi screen, robust seed correction, and bioinformatics analysis to help identify genes that could potentiate SMN expression in combination with currently approved treatments. Based on the rigorous nature of our screening strategy, we identified a small list of genes and pathways that are likely to alter SMN gene expression through induction of transcription, RNA processing, and post-translational modifications.

Transcriptional regulation of SMN expression

Very little is known about the regulatory mechanisms regulating *SMN1* and *SMN2* promoter activity, despite several reports describing differential SMN expression in varying tissues throughout development (Echaniz-Laguna et al., 1999; Monani et al., 1999b; Ramos et al., 2019; Rouget et al., 2005). Putative consensus binding sites for the transcriptional repressor YY1 were previously described in the *SMN2* promoter (Echaniz-Laguna et al., 1999). YY1 was a highly ranked hit from our current screen and the highest ranked transcription factor. YY1 is thought to induce transcriptional repression by directing the activity of

HDACs at gene promoters. Intriguingly, HDAC inhibitors have been shown to increase SMN expression and were previously under clinical consideration for treating SMA (Kissel et al., 2011, 2014; Krossschell et al., 2018; Renusch et al., 2015; Swoboda et al., 2009, 2010). Although numerous off-target effects precluded further clinical consideration of this class of drug, it is possible that identifying transcription factors could provide another avenue for therapeutic intervention in this pathway.

STRING analysis showed several transcription factors clustered around YY1, including HCFC1, GABP, and SUZ12. HCFC1 gain- and loss-of-function mutations have been described in neurodevelopmental disorders, suggesting it plays critical roles in central nervous system development (Gérard et al., 2015; Koufaris et al., 2016; Yu et al., 2013). HCFC1 associates with DNA-binding transcription factors and chromatin modifiers to either activate or repress transcription. One report estimates that close to 90% of promoters that HCFC1 binds to also bind YY1 or GABP (Michaud et al., 2013). Association of GABP with HCFC1 is thought to be essential for HCFC1 to regulate the transcription of several genes (Michaud et al., 2013). Knocking down YY1, GABP, or HCFC1 individually increases SMN expression, suggesting a critical role in SMN transcriptional induction. Therapies that increase SMN exon 7 inclusion are limited by the level of expression of the SMN2 transcript. Identifying pathways that could be targeted to increase the levels of SMN transcript would provide a mechanism to complement the splicing modifiers to further increase SMN expression.

SMN2 splicing modifiers

Outside of replacing the *SMN1* gene, maximizing the production of the SMN protein from the *SMN2* gene has been the primary therapeutic focus of SMA research. Indeed, one clinically approved treatment for SMA leveraged the discovery of the intronic splicing silencer N1 (ISS-N1) to design antisense oligonucleotides that target this site to suppress SMN exon 7 skipping (Singh et al., 2006). Subsequently, small-molecule screens have identified compounds that promote SMN exon 7 inclusion, and several of these entities are currently under advanced clinical examination (Cheung et al., 2018; Poirier et al., 2018; Ratni et al., 2018; Sturm et al., 2019). Although promoting SMN exon 7 inclusion has remarkable therapeutic benefits, antisense oligonucleotides targeting ISS-N1 do not help all patients, possibly because the splice sites harbor sequence variants that could render them nonfunctional. This fundamental gap in knowledge of the molecular mechanisms regulating SMN splicing prevents additional mechanism-based drug development to further enhance the efficacy of this class of drug.

To date, only a few proteins have been shown to reduce or increase SMN exon 7 inclusion in knockdown and overexpression studies. The C-to-T transition at position 6 in SMN2 exon 7 is thought to alter the delicate balance between multiple positive and negative splicing modulators (Lorson et al., 1999; Singh and Singh, 2018). SRSF1, a member of the family of serine/arginine (SR)-rich proteins, was shown to increase exon 7 inclusion when knocked down or overexpressed, suggesting a complicated role in SMN splicing (Cartegni and Krainer, 2002; Kashima and Manley, 2003; Wee et al., 2014). hnRNP A1/A2 depletion enhances exon 7 inclusion, suggesting an inhibitory role in SMN exon 7 inclusion (Doktor

et al., 2011; Kashima et al., 2007a, 2007b; Singh et al., 2013, 2017). In this study, knocking down SRSF3 or hnRNP A1 increases full-length SMN expression consistent with previous findings. We also re-identified U2AF1 and PUF60 that have been previously reported to suppress SMN exon 7 inclusion (Auslander et al., 2020; Hastings et al., 2007). Together, we found that siRNA targeting almost all the previously confirmed genes that promote SMN exon 7 exclusion is indicative of the robustness of the screening strategy.

Nuclear transport of SMN RNA mediates SMN expression

Prior research on stimulating SMN gene expression through the *SMN2*-derived mRNA has focused on increasing mRNA synthesis, correcting the splicing to promote exon 7 inclusion, or slowing RNA metabolism (Avila et al., 2007; Farooq et al., 2011, 2013; Hua et al., 2008, 2011; Sumner et al., 2003). Increasing evidence suggests that the export of mRNA is a key regulator of gene expression and selective mRNA export (García-Oliver et al., 2012; Wickramasinghe and Laskey, 2015). Here, we provide evidence that increased export of *SMN2* mRNA into the cytoplasm leads to increased SMN protein levels, suggesting an additional mechanism to increase SMN protein.

In mammalian cells, pre-mRNA transcripts are recognized by the CPSF complex, which, through recognition of the hexanucleotide A(A/U)UAAA motif within polyadenylation signals, catalyzes pre-mRNA cleavage and initiates polyadenylation (Schönemann et al., 2014). WDR33, CPSF4, FIP1L1, and CPSF1 are core components of the CPSF complex, which have discrete roles in RNA recognition and maturation. CPSF1 and WDR33 form a heterodimer, independently of the other CPSF subunits, and are required and sufficient for recognition of the polyadenylation motif. In this study, we found that knocking down CPSF1 and WDR33, but not CPSF4 and FIP1L1, increased SMN expression, in line with the indispensable roles of CPSF1 and WDR33 in hexanucleotide recognition and binding. Nevertheless, it is unclear why reducing key components of mRNA biogenesis would result in increased expression of the SMN protein. Further exploration revealed that knocking down WDR33, but not CPSF1 or THOC3, altered the levels of SMN pre-mRNA, whereas none of the knockdowns affected the stability of SMN mRNA. Intriguingly, knocking down WDR33, CPSF1, and THOC3 resulted in increased cytoplasmic SMN transcript, suggesting that cytoplasmic trafficking of SMN mRNA was enhanced when each gene is depleted.

The THO/TREX complex is recruited to maturing RNA and facilitates nuclear export of a subset of mRNAs to the cytoplasm for translation (Guria et al., 2011). In the current study, we found that siRNA targeting core components of the THO/TREX complex reduced SMN expression, as expected. However, transient silencing of THOC3 resulted in increased cytoplasmic localization of SMN mRNA and increased SMN protein expression. Silencing of THOC3 has been previously reported to both increase and decrease expression of genes, suggesting tissue-specific, condition-dependent, and temporal roles in gene expression (Gupta and Senthilkumaran, 2020). This sets up the intriguing possibility that SMN mRNA nucleocytoplasmic trafficking could be one factor that drives the tissue-dependent and developmental variability in SMN protein expression in disease-relevant tissues, including motor neurons and muscle.

Regulators of SMN protein turnover

We and others have shown that SMN protein is targeted for degradation by the ubiquitin-proteasome system (Abera et al., 2016; Chang et al., 2004; Kwon et al., 2011, 2013). In this study, we show that siRNA targeting enzymes that catalyze protein ubiquitination or the substrate recognition domains of the proteasome increase SMN levels, consistent with our previous findings. We identified an additional E3 ligase, *Neur12*, which promotes SMN ubiquitination and its subsequent degradation. *Neur12* ubiquitinates SMN directly *in vitro* and in cultured cells. We show that *Neur12* is required for Mib1-dependent SMN ubiquitination and turnover, adding an additional layer of post-translational gene regulation. We have previously shown that a small-molecule inhibitor of SMN ubiquitination by Mib1 increases SMN levels and improves the SMA phenotype in a severe mouse model of SMA (Abera et al., 2016). Although studies to identify a clinical candidate that inhibits Mib1-dependent SMN turnover remain ongoing in our lab, finding additional genes that could potentially be more druggable is prudent.

Conclusions

Many human diseases are caused by toxic accumulation of proteins or the inappropriate clearance of proteins resulting in functional deficits. The genes and pathways that regulate the delicate balance between gene transcription and protein degradation have been difficult to identify because of the number of molecular steps involved and the inherent redundancy involved in maintaining protein homeostasis. High-throughput genome-wide gene suppression assays are ideal to begin identifying critical proteins involved in selectively regulating steady-state levels of disease-associated proteins. Using this strategy, we have identified genes that have not previously been implicated in regulating SMN protein levels. We validated several of the hits in SMA patient-derived cells and provided initial molecular characterization of their modes of action.

STAR★METHODS

Detailed methods are provided in the online version of this paper and include the following:

RESOURCE AVAILABILITY

Lead contact—Further information and requests for resources and reagents should be directed to and will be fulfilled by the Lead Contact, Barrington Burnett (barrington.burnett@usuhs.edu).

Materials availability—Plasmids generated in this study are available from the lead contact by request.

Data and code availability—The accession number for the genome-wide RNAi screen dataset reported in this paper is PubChem: 1347426.

EXPERIMENTAL MODEL AND SUBJECT DETAILS

Cell culture—3813 fibroblasts derived from an SMA patient were maintained in DMEM supplemented with 10% fetal bovine serum and 1% Pencicillin-Streptomycin Glutamine. Cells were incubated at 37°C with 5% CO₂.

METHOD DETAILS

Plasmids—We generated HA-Neurl2 constructs that were not targets of the Neurl2 siRNA (Thermo Fisher, Assay ID: s44413). Neurl2res was generated by introducing silent mutations in the siRNA-targeting region (T702G, C705T, A708C, and G711A) of HA-tagged Neurl2 constructs.

siRNA screening—*SMN2*-HEK-luciferase reporter cells were reverse transfected with siRNAs in 384-well optical plates (2 µL per well, 0.8 pmol). Each well contained, 20 µL of DMEM medium and 4 µl/ml RNAiMAX. After 30 min incubation, 20 µL of a 37,500 cells per ml suspension was added to each well for reverse transfection. Plates with cells were incubated at 37°C/5% CO₂ for a further 72 h. Media was DMEM supplemented with luciferin (1 µM) and B-27 supplement, and the plates were sealed with an optically clear film. Plates were incubated at 37°C incubator and bioluminescence recorded with a PE ViewLux. Pilot and primary screens were similarly performed with a unique set of siRNAs performed. All screens were performed in temperature-controlled enclosures with automated liquid and plate handling. Luciferase signals were normalized to Ambion Silencer Negative Control #2 siRNA, then log₁₀ transformed to achieve normal distribution.

STRING analysis—Gene Ontology (GO) enrichment analysis of the top genes that increased or decreased SMN expression was performed with the “cellular components enrichment” tool of the STRING database (<https://string-db.org/>). Statistical significance for enrichment by genome-wide false discovery rate (FDR) was calculated using the STRING database (Szklarczyk et al., 2017).

RNAi screen validation—250,000 fibroblasts were plated and transfected with 30 pmol siRNA using Lipofectamine RNAiMAX in Opti-MEM. Cells were collected 48 hours after transfection for further analysis. siRNAs were all purchased from Thermo Fisher. An siRNA-resistant form of Neurl2 was generated by introducing silent mutations in the siRNA-targeting region (G750A, A753C, G756A, and C759T) of HA-tagged Neurl2 cDNA construct using site-directed mutagenesis. Mib1 was overexpressed using a previously described FLAG-Mib1 plasmid (Itoh et al., 2003).

Protein expression analysis—Cells were lysed in 1% NP-40, 50 mM Tris-HCl (pH 8.0), 150 mM NaCl, and protease inhibitor cocktail on ice for 10 minutes. Protein concentrations were determined using a DC assay according to the manufacturer’s protocol. Protein lysates were resolved by 4%–12% SDS-PAGE and transferred to PVDF membranes. Membranes were blocked in 5% milk in TBST for 1 hour at room temperature. Membranes were incubated with primary antibody (mouse anti-SMN, 1:1000) followed by incubation in secondary antibody. Mouse anti-β-actin peroxidase was used as a loading control. Western blots were quantified using ImageJ.

RNA isolation and gene expression analysis—Total RNA was extracted using the QIAzol-chloroform method as previously described. RNA was purified using the RNeasy kit using the manufacturer's instructions. cDNA was synthesized from one microgram of RNA using the High-Capacity cDNA Reverse Transcriptase Kit. qRT-PCR was performed using Taqman reagents and TaqMan primers were all purchased from Thermo Fisher.

SMN pre-mRNA—SMN pre-mRNA levels were determined as previously described (d'Ydewalle et al., 2017). Briefly, SMN pre-mRNA was amplified using reverse transcriptase and a strand specific primer. RT-PCR was used to determine relative SMN pre-mRNA levels using TaqMan reagents and a custom TaqMan primer.

SMN2 mRNA splicing—*SMN2* transcripts were amplified from cDNA using PCR SuperMix. PCR products were run on a 2% agarose gel at 150 V for 30 minutes. The full-length SMN (421 bp) and the SMN 7 (367 bp) products were quantified using ImageJ. The ratio of full-length SMN to SMN 7 was calculated.

mRNA stability—Actinomycin D (5 µg/mL) was added to cells 48 hours after transfection with siRNA. Cells were collected 0, 1, 3, 5, and 8 hours after the addition of actinomycin D. RNA was extracted and purified from cells and then transcribed into cDNA. Relative *SMN* mRNA levels over time were determined using qRT-PCR.

mRNA Fractionation—The SurePrep Nuclear or Cytoplasmic RNA Purification Kit was used for mRNA fractionation. Briefly, cells were lysed using the provided lysis solution and the lysate was spun down for 3 minutes at maximum speed in a benchtop centrifuge to separate the nuclear and cytoplasmic fractions. Cytoplasmic mRNA was isolated from the supernatant and nuclear mRNA was isolated from the pellet. cDNA was synthesized from one microgram of RNA using the High Capacity cDNA Reverse Transcriptase Kit. qRT-PCR was performed using Taqman reagents and TaqMan primers were all purchased from Thermo Fisher. Nuclear SMN2 mRNA expression was normalized to MALAT1 mRNA and cytoplasmic SMN2 mRNA expression was normalized to ACTB mRNA. Purity of nuclear and cytoplasmic fractions was confirmed by examining expression of ACTB and MALAT1 mRNA using qRT-PCR.

Immunoprecipitation—Fibroblasts were transfected with either GFP-Neur12 or Neur12-GFP constructs. SMN was immunoprecipitated using an anti-SMN antibody and samples were resolved by 4%–12% SDS-PAGE. Western blots were probed with an anti-GFP antibody.

***In vitro* ubiquitination**—*In vitro* ubiquitination reactions were performed as previously described (Kwon et al., 2013). Briefly, recombinant SMN protein was incubated with ubiquitin, an E1 ubiquitin-activating enzyme, an E2 ubiquitin-conjugating enzyme, and recombinant Mib1 or Neur12 in reaction buffer (50 mM Tris-HCl, pH 7.5, 2 mM ATP, 4 mM MgCl₂, 2 mM dithiothreitol (DTT)) for 1 hour at 37°C. Reactions were quenching with 5X Laemmli sample buffer, boiled for 5 minutes, and separated via SDS-PAGE. Western blots were probed with an antibody against polyubiquitin.

Pulse-chase protein labeling—Pulse-chase analysis was performed as previously described (Burnett et al., 2009). Briefly, fibroblasts derived from patients with SMA were incubated in cysteine-methionine-free medium for 2 h followed by incubation in methionine-free medium containing 100 μ Ci of 35 S-labeled cysteine-methionine for 1 h. After labeling, cells were washed with culture medium containing an excess of unlabeled cysteine and methionine and then further incubated with the same medium. Cells were collected at the indicated time points. SMN was immunoprecipitated using an anti-SMN antibody. Samples were separated on SDS-10% PAGE which were then dried and exposed to a phosphorimager screen. The signal was visualized using a Storm phosphorimager system. Densitometry analysis of SMN protein bands was carried out using ImageQuant PhosphorImager software.

QUANTIFICATION AND STATISTICAL ANALYSIS

All experiments were repeated at least three times, and quantitative data are presented as the mean \pm SEM. All statistical analyses were performed using GraphPad Prism v7.05. Outliers were determined using Grubbs' test where $\alpha = 0.05$. The distribution of data points was assessed using the Shapiro-Wilk normality test and homogeneity of variances was assessed using either an F test or a Brown-Forsythe test. Data were analyzed using either an unpaired t test (for comparisons with one independent variable and 2 groups), or a one-way analysis of variance (ANOVA; for comparisons with one independent variable and > 2 groups). *Post hoc* analyses were performed using either Dunnett's or Tukey's multiple comparisons test. A *p* value < 0.05 was considered statistically significant.

Supplementary Material

Refer to Web version on PubMed Central for supplementary material.

ACKNOWLEDGMENTS

This work was supported by a research grant to B.G.B. from the National Institute of Neurological Disorders and Stroke at the NIH (R01NS091575).

REFERENCES

- Abera MB, Xiao J, Nofziger J, Titus S, Southall N, Zheng W, Moritz KE, Ferrer M, Cherry JJ, Androphy EJ, et al. (2016). ML372 blocks SMN ubiquitination and improves spinal muscular atrophy pathology in mice. *JCI Insight* 1, e88427. [PubMed: 27882347]
- Amm I, Sommer T, and Wolf DH (2014). Protein quality control and elimination of protein waste: the role of the ubiquitin-proteasome system. *Biochim. Biophys. Acta* 1843, 182–196. [PubMed: 23850760]
- Aragon-Gawinska K, Daron A, Ulinici A, Vanden Brande L, Seferian A, Gidaro T, Scoto M, Deconinck N, and Servais L; SMA-Registry Study Group (2020). Sitting in patients with spinal muscular atrophy type 1 treated with nusinersen. *Dev. Med. Child Neurol.* 62, 310–314. [PubMed: 31799720]
- Auslander N, Ramos DM, Zelaya I, Karathia H, Crawford TO, Schäffer AA, Sumner CJ, and Ruppin E (2020). The GENDULF algorithm: mining transcriptomics to uncover modifier genes for monogenic diseases. *Mol. Syst. Biol.* 16, e9701. [PubMed: 33438800]
- Avila AM, Burnett BG, Taye AA, Gabanella F, Knight MA, Hartenstein P, Cizman Z, Di Prospero NA, Pellizzoni L, Fischbeck KH, and Sumner CJ (2007). Trichostatin A increases SMN expression

- and survival in a mouse model of spinal muscular atrophy. *J. Clin. Invest.* 117, 659–671. [PubMed: 17318264]
- Buehler E, Khan AA, Marine S, Rajaram M, Bahl A, Burchard J, and Ferrer M (2012). siRNA off-target effects in genome-wide screens identify signaling pathway members. *Sci. Rep.* 2, 428. [PubMed: 22645644]
- Burnett BG, Muñoz E, Tandon A, Kwon DY, Sumner CJ, and Fischbeck KH (2009). Regulation of SMN protein stability. *Mol. Cell. Biol.* 29, 1107–1115. [PubMed: 19103745]
- Cartegni L, and Krainer AR (2002). Disruption of an SF2/ASF-dependent exonic splicing enhancer in SMN2 causes spinal muscular atrophy in the absence of SMN1. *Nat. Genet.* 30, 377–384. [PubMed: 11925564]
- Chan S, Choi EA, and Shi Y (2011). Pre-mRNA 3'-end processing complex assembly and function. *Wiley Interdiscip. Rev. RNA* 2, 321–335. [PubMed: 21957020]
- Chang HC, Hung WC, Chuang YJ, and Jong YJ (2004). Degradation of survival motor neuron (SMN) protein is mediated via the ubiquitin/proteasome pathway. *Neurochem. Int.* 45, 1107–1112. [PubMed: 15337310]
- Cheung AK, Hurley B, Kerrigan R, Shu L, Chin DN, Shen Y, O'Brien G, Sung MJ, Hou Y, Axford J, et al. (2018). Discovery of Small Molecule Splicing Modulators of Survival Motor Neuron-2 (SMN2) for the Treatment of Spinal Muscular Atrophy (SMA). *J. Med. Chem.* 61, 11021–11036. [PubMed: 30407821]
- Chung N, Zhang XD, Kreamer A, Locco L, Kuan PF, Bartz S, Linsley PS, Ferrer M, and Strulovici B (2008). Median absolute deviation to improve hit selection for genome-scale RNAi screens. *J. Biomol. Screen.* 13, 149–158. [PubMed: 18216396]
- d'Ydewalle C, Ramos DM, Pyles NJ, Ng SY, Gorz M, Pilato CM, Ling K, Kong L, Ward AJ, Rubin LL, et al. (2017). The Antisense Transcript SMN-AS1 Regulates SMN Expression and Is a Novel Therapeutic Target for Spinal Muscular Atrophy. *Neuron* 93, 66–79. [PubMed: 28017471]
- Doktor TK, Schroeder LD, Vestad A, Palmfeldt J, Andersen HS, Gregersen N, and Andresen BS (2011). SMN2 exon 7 splicing is inhibited by binding of hnRNP A1 to a common ESS motif that spans the 3' splice site. *Hum. Mutat.* 32, 220–230. [PubMed: 21120954]
- Echaniz-Laguna A, Miniou P, Bartholdi D, and Melki J (1999). The promoters of the survival motor neuron gene (SMN) and its copy (SMNc) share common regulatory elements. *Am. J. Hum. Genet.* 64, 1365–1370. [PubMed: 10205267]
- Farooq F, Molina FA, Hadwen J, MacKenzie D, Witherspoon L, Osmond M, Holcik M, and MacKenzie A (2011). Prolactin increases SMN expression and survival in a mouse model of severe spinal muscular atrophy via the STAT5 pathway. *J. Clin. Invest.* 121, 3042–3050. [PubMed: 21785216]
- Farooq F, Abadía-Molina F, MacKenzie D, Hadwen J, Shamim F, O'Reilly S, Holcik M, and MacKenzie A (2013). Celecoxib increases SMN and survival in a severe spinal muscular atrophy mouse model via p38 pathway activation. *Hum. Mol. Genet.* 22, 3415–3424. [PubMed: 23656793]
- Finkel RS, Mercuri E, Darras BT, Connolly AM, Kuntz NL, Kirschner J, Chiriboga CA, Saito K, Servais L, Tizzano E, et al. ; ENDEAR Study Group (2017). Nusinersen versus Sham Control in Infantile-Onset Spinal Muscular Atrophy. *N. Engl. J. Med.* 377, 1723–1732. [PubMed: 29091570]
- Foust KD, Wang X, McGovern VL, Braun L, Bevan AK, Haidet AM, Le TT, Morales PR, Rich MM, Burghes AH, and Kaspar BK (2010). Rescue of the spinal muscular atrophy phenotype in a mouse model by early postnatal delivery of SMN. *Nat. Biotechnol.* 28, 271–274. [PubMed: 20190738]
- García-Oliver E, García-Molinero V, and Rodríguez-Navarro S (2012). mRNA export and gene expression: the SAGA-TREX-2 connection. *Biochim. Biophys. Acta* 1819, 555–565. [PubMed: 22178374]
- Gérard M, Morin G, Bourillon A, Colson C, Mathieu S, Rabier D, Billette de Villemeur T, Ogier de Baulny H, and Benoist JF (2015). Multiple congenital anomalies in two boys with mutation in HCFC1 and cobalamin disorder. *Eur. J. Med. Genet.* 58, 148–153.
- Gray KM, Kaifer KA, Baillat D, Wen Y, Bonacci TR, Ebert AD, Raimer AC, Spring AM, Have ST, Glascock JJ, et al. (2018). Self-oligomerization regulates stability of survival motor neuron protein isoforms by sequestering an SCF^{S^{lmb}} degron. *Mol. Biol. Cell* 29, 96–110. [PubMed: 29167380]

- Gupta YR, and Senthilkumaran B (2020). Identification, expression profiling and localization of thoc in common carp ovary: Influence of thoc3-siRNA transient silencing. *Gene* 732, 144350. [PubMed: 31935505]
- Guria A, Tran DD, Ramachandran S, Koch A, El Bounkari O, Dutta P, Hauser H, and Tamura T (2011). Identification of mRNAs that are spliced but not exported to the cytoplasm in the absence of THOC5 in mouse embryo fibroblasts. *RNA* 17, 1048–1056. [PubMed: 21525145]
- Han KJ, Foster DG, Zhang NY, Kanisha K, Dzieciatkowska M, Sclafani RA, Hansen KC, Peng J, and Liu CW (2012). Ubiquitin-specific protease 9x deubiquitinates and stabilizes the spinal muscular atrophy protein-survival motor neuron. *J. Biol. Chem.* 287, 43741–43752. [PubMed: 23112048]
- Hastings ML, Allemand E, Duelli DM, Myers MP, and Krainer AR (2007). Control of pre-mRNA splicing by the general splicing factors PUF60 and U2AF(65). *PLoS ONE* 2, e538. [PubMed: 17579712]
- Heath CG, Viphakone N, and Wilson SA (2016). The role of TREX in gene expression and disease. *Biochem. J.* 473, 2911–2935. [PubMed: 27679854]
- Hofmann Y, Lorson CL, Stamm S, Androphy EJ, and Wirth B (2000). Htra2-beta 1 stimulates an exonic splicing enhancer and can restore full-length SMN expression to survival motor neuron 2 (SMN2). *Proc. Natl. Acad. Sci. USA* 97, 9618–9623. [PubMed: 10931943]
- Hsu SH, Lai MC, Er TK, Yang SN, Hung CH, Tsai HH, Lin YC, Chang JG, Lo YC, and Jong YJ (2010). Ubiquitin carboxyl-terminal hydrolase L1 (UCHL1) regulates the level of SMN expression through ubiquitination in primary spinal muscular atrophy fibroblasts. *Clin. Chim. Acta* 411, 1920–1928. [PubMed: 20713032]
- Hua Y, Vickers TA, Okunola HL, Bennett CF, and Krainer AR (2008). Antisense masking of an hnRNP A1/A2 intronic splicing silencer corrects SMN2 splicing in transgenic mice. *Am. J. Hum. Genet.* 82, 834–848. [PubMed: 18371932]
- Hua Y, Sahashi K, Rigo F, Hung G, Horev G, Bennett CF, and Krainer AR (2011). Peripheral SMN restoration is essential for long-term rescue of a severe spinal muscular atrophy mouse model. *Nature* 478, 123–126. [PubMed: 21979052]
- Itoh M, Kim CH, Palardy G, Oda T, Jiang YJ, Maust D, Yeo SY, Lorick K, Wright GJ, Ariza-McNaughton L, et al. (2003). Mind bomb is a ubiquitin ligase that is essential for efficient activation of Notch signaling by Delta. *Dev. Cell* 4, 67–82. [PubMed: 12530964]
- Kaifer KA, Villalón E, Osman EY, Glascock JJ, Arnold LL, Cornelison DDW, and Lorson CL (2017). Plastin-3 extends survival and reduces severity in mouse models of spinal muscular atrophy. *JCI Insight* 2, e89970. [PubMed: 28289706]
- Kashima T, and Manley JL (2003). A negative element in SMN2 exon 7 inhibits splicing in spinal muscular atrophy. *Nat. Genet.* 34, 460–463. [PubMed: 12833158]
- Kashima T, Rao N, David CJ, and Manley JL (2007a). hnRNP A1 functions with specificity in repression of SMN2 exon 7 splicing. *Hum. Mol. Genet.* 16, 3149–3159. [PubMed: 17884807]
- Kashima T, Rao N, and Manley JL (2007b). An intronic element contributes to splicing repression in spinal muscular atrophy. *Proc. Natl. Acad. Sci. USA* 104, 3426–3431. [PubMed: 17307868]
- Katahira J (2012). mRNA export and the TREX complex. *Biochim. Biophys. Acta* 1819, 507–513. [PubMed: 22178508]
- Kelly WK, O'Connor OA, and Marks PA (2002). Histone deacetylase inhibitors: from target to clinical trials. *Expert Opin. Investig. Drugs* 11, 1695–1713.
- Kissel JT, Scott CB, Reyna SP, Crawford TO, Simard LR, Krossschell KJ, Acsadi G, Elsheik B, Schroth MK, D'Anjou G, et al. ; Project Cure Spinal Muscular Atrophy Investigators' Network (2011). SMA CARNIVAL TRIAL PART II: a prospective, single-armed trial of L-carnitine and valproic acid in ambulatory children with spinal muscular atrophy. *PLoS ONE* 6, e21296. [PubMed: 21754985]
- Kissel JT, Elsheikh B, King WM, Freimer M, Scott CB, Kolb SJ, Reyna SP, Crawford TO, Simard LR, Krossschell KJ, et al. ; Project Cure Spinal Muscular Atrophy Investigators Network (2014). SMA valiant trial: a prospective, double-blind, placebo-controlled trial of valproic acid in ambulatory adults with spinal muscular atrophy. *Muscle Nerve* 49, 187–192. [PubMed: 23681940]

- Koufaris C, Alexandrou A, Tanteles GA, Anastasiadou V, and Sismani C (2016). A novel *HCFC1* variant in male siblings with intellectual disability and microcephaly in the absence of cobalamin disorder. *Biomed. Rep.* 4, 215–218. [PubMed: 26893841]
- Krosschell KJ, Kissel JT, Townsend EL, Simeone SD, Zhang RZ, Reyna SP, Crawford TO, Schroth MK, Acsadi G, Kishnani PS, et al. ; Project Cure SMA Investigator's Network (2018). Clinical trial of L-Carnitine and valproic acid in spinal muscular atrophy type I. *Muscle Nerve* 57, 193–199. [PubMed: 28833236]
- Kwon DY, Motley WW, Fischbeck KH, and Burnett BG (2011). Increasing expression and decreasing degradation of SMN ameliorate the spinal muscular atrophy phenotype in mice. *Hum. Mol. Genet.* 20, 3667–3677. [PubMed: 21693563]
- Kwon DY, Dimitriadi M, Terzic B, Cable C, Hart AC, Chitnis A, Fischbeck KH, and Burnett BG (2013). The E3 ubiquitin ligase mind bomb 1 ubiquitinates and promotes the degradation of survival of motor neuron protein. *Mol. Biol. Cell* 24, 1863–1871. [PubMed: 23615451]
- Lefebvre S, Bürglen L, Reboullet S, Clermont O, Burlet P, Viollet L, Benichou B, Cruaud C, Millasseau P, Zeviani M, et al. (1995). Identification and characterization of a spinal muscular atrophy-determining gene. *Cell* 80, 155–165. [PubMed: 7813012]
- Locatelli D, Terao M, Kurosaki M, Zanellati MC, Pletto DR, Finardi A, Colciaghi F, Garattini E, and Battaglia GS (2015). Different Stability and Proteasome-Mediated Degradation Rate of SMN Protein Isoforms. *PLoS ONE* 10, e0134163. [PubMed: 26214005]
- Lorson CL, Hahnen E, Androphy EJ, and Wirth B (1999). A single nucleotide in the SMN gene regulates splicing and is responsible for spinal muscular atrophy. *Proc. Natl. Acad. Sci. USA* 96, 6307–6311. [PubMed: 10339583]
- Mailman MD, Heinz JW, Papp AC, Snyder PJ, Sedra MS, Wirth B, Burghes AH, and Prior TW (2002). Molecular analysis of spinal muscular atrophy and modification of the phenotype by SMN2. *Genet. Med.* 4, 20–26. [PubMed: 11839954]
- Marine S, Bahl A, Ferrer M, and Buehler E (2012). Common seed analysis to identify off-target effects in siRNA screens. *J. Biomol. Screen.* 17, 370–378. [PubMed: 22086724]
- Martins de Araújo M, Bonnal S, Hastings ML, Krainer AR, and Valcárcel J (2009). Differential 3' splice site recognition of SMN1 and SMN2 transcripts by U2AF and U2 snRNP. *RNA* 15, 515–523. [PubMed: 19244360]
- Mason PB, and Struhl K (2005). Distinction and relationship between elongation rate and processivity of RNA polymerase II in vivo. *Mol. Cell* 17, 831–840. [PubMed: 15780939]
- Mendell JR, Al-Zaidy S, Shell R, Arnold WD, Rodino-Klapac LR, Prior TW, Lowes L, Alfano L, Berry K, Church K, et al. (2017). Single-Dose Gene-Replacement Therapy for Spinal Muscular Atrophy. *N. Engl. J. Med.* 377, 1713–1722. [PubMed: 29091557]
- Mercuri E, Darras BT, Chiriboga CA, Day JW, Campbell C, Connolly AM, Iannaccone ST, Kirschner J, Kuntz NL, Saito K, et al. ; CHERISH Study Group (2018). Nusinersen versus Sham Control in Later-Onset Spinal Muscular Atrophy. *N. Engl. J. Med.* 378, 625–635. [PubMed: 29443664]
- Michaud J, Praz V, James Faresse N, Jnbaptiste CK, Tyagi S, Schütz F, and Herr W (2013). *HCFC1* is a common component of active human CpG-island promoters and coincides with ZNF143, THAP11, YY1, and GABP transcription factor occupancy. *Genome Res.* 23, 907–916. [PubMed: 23539139]
- Monani UR, Lorson CL, Parsons DW, Prior TW, Androphy EJ, Burghes AH, and McPherson JD (1999a). A single nucleotide difference that alters splicing patterns distinguishes the SMA gene SMN1 from the copy gene SMN2. *Hum. Mol. Genet.* 8, 1177–1183. [PubMed: 10369862]
- Monani UR, McPherson JD, and Burghes AH (1999b). Promoter analysis of the human centromeric and telomeric survival motor neuron genes (SMNC and SMNT). *Biochim. Biophys. Acta* 1445, 330–336. [PubMed: 10366716]
- Oprea GE, Kröber S, McWhorter ML, Rossoll W, Müller S, Krawczak M, Bassell GJ, Beattie CE, and Wirth B (2008). Plastin 3 is a protective modifier of autosomal recessive spinal muscular atrophy. *Science* 320, 524–527. [PubMed: 18440926]
- Passini MA, Bu J, Roskelley EM, Richards AM, Sardi SP, O'Riordan CR, Klinger KW, Shihabuddin LS, and Cheng SH (2010). CNS-targeted gene therapy improves survival and motor function in a mouse model of spinal muscular atrophy. *J. Clin. Invest.* 120, 1253–1264. [PubMed: 20234094]

- Pazin MJ, and Kadonaga JT (1997). What's up and down with histone deacetylation and transcription? *Cell* 89, 325–328. [PubMed: 9150131]
- Pellizzoni LYong J, and Dreyfuss G (2002). Essential role for the SMN complex in the specificity of snRNP assembly. *Science* 298, 1775–1779. [PubMed: 12459587]
- Poirier A, Weetall M, Heinig K, Bucheli F, Schoenlein K, Alsenz J, Bassett S, Ullah M, Senn C, Ratni H, et al. (2018). Risdiplam distributes and increases SMN protein in both the central nervous system and peripheral organs. *Pharmacol. Res. Perspect.* 6, e00447. [PubMed: 30519476]
- Powis RA, Karyka E, Boyd P, Côme J, Jones RA, Zheng Y, Szunyogova E, Groen EJ, Hunter G, Thomson D, et al. (2016). Systemic restoration of UBA1 ameliorates disease in spinal muscular atrophy. *JCI Insight* 1, e87908. [PubMed: 27699224]
- Ramos DM, d'Ydewalle C, Gabbeta V, Dakka A, Klein SK, Norris DA, Matson J, Taylor SJ, Zaworski PG, Prior TW, et al. (2019). Age-dependent SMN expression in disease-relevant tissue and implications for SMA treatment. *J. Clin. Invest.* 129, 4817–4831. [PubMed: 31589162]
- Ramser J, Ahearn ME, Lenski C, Yariz KO, Hellebrand H, von Rhein M, Clark RD, Schmutzler RK, Lichtner P, Hoffman EP, et al. (2008). Rare missense and synonymous variants in UBE1 are associated with X-linked infantile spinal muscular atrophy. *Am. J. Hum. Genet.* 82, 188–193. [PubMed: 18179898]
- Ratni H, Ebeling M, Baird J, Bendels S, Bylund J, Chen KS, Denk N, Feng Z, Green L, Guerard M, et al. (2018). Discovery of Risdiplam, a Selective Survival of Motor Neuron-2 (SMN2) Gene Splicing Modifier for the Treatment of Spinal Muscular Atrophy (SMA). *J. Med. Chem.* 61, 6501–6517. [PubMed: 30044619]
- Renusch SR, Harshman S, Pi H, Workman E, Wehr A, Li X, Prior TW, Elsheikh BH, Swoboda KJ, Simard LR, et al. (2015). Spinal Muscular Atrophy Biomarker Measurements from Blood Samples in a Clinical Trial of Valproic Acid in Ambulatory Adults. *J. Neuromuscul. Dis.* 2, 119–130. [PubMed: 27858735]
- Riessland M, Kaczmarek A, Schneider S, Swoboda KJ, Löhr H, Bradler C, Grysko V, Dimitriadi M, Hosseinibarkoobe S, Torres-Benito L, et al. (2017). Neurocalcin Delta Suppression Protects against Spinal Muscular Atrophy in Humans and across Species by Restoring Impaired Endocytosis. *Am. J. Hum. Genet.* 100, 297–315. [PubMed: 28132687]
- Rouget R, Vigneault F, Codio C, Rochette C, Paradis I, Drouin R, and Simard LR (2005). Characterization of the survival motor neuron (SMN) promoter provides evidence for complex combinatorial regulation in undifferentiated and differentiated P19 cells. *Biochem. J.* 385, 433–443. [PubMed: 15361068]
- Schönemann L, Kühn U, Martin G, Schäfer P, Gruber AR, Keller W, Zavolan M, and Wahle E (2014). Reconstitution of CPSF active in polyadenylation: recognition of the polyadenylation signal by WDR33. *Genes Dev.* 28, 2381–2393. [PubMed: 25301781]
- Singh RN, and Singh NN (2018). Mechanism of Splicing Regulation of Spinal Muscular Atrophy Genes. *Adv. Neurobiol.* 20, 31–61. [PubMed: 29916015]
- Singh NK, Singh NN, Androphy EJ, and Singh RN (2006). Splicing of a critical exon of human Survival Motor Neuron is regulated by a unique silencer element located in the last intron. *Mol. Cell. Biol.* 26, 1333–1346. [PubMed: 16449646]
- Singh NN, Seo J, Ottesen EW, Shishimorova M, Bhattacharya D, and Singh RN (2011). TIA1 prevents skipping of a critical exon associated with spinal muscular atrophy. *Mol. Cell. Biol.* 31, 935–954. [PubMed: 21189287]
- Singh NN, Lawler MN, Ottesen EW, Upreti D, Kaczynski JR, and Singh RN (2013). An intronic structure enabled by a long-distance interaction serves as a novel target for splicing correction in spinal muscular atrophy. *Nucleic Acids Res.* 41, 8144–8165. [PubMed: 23861442]
- Singh NN, Del Rio-Malewski JB, Luo D, Ottesen EW, Howell MD, and Singh RN (2017). Activation of a cryptic 5' splice site reverses the impact of pathogenic splice site mutations in the spinal muscular atrophy gene. *Nucleic Acids Res.* 45, 12214–12240. [PubMed: 28981879]
- Song R, Koo BK, Yoon KJ, Yoon MJ, Yoo KW, Kim HT, Oh HJ, Kim YY, Han JK, Kim CH, and Kong YY (2006). Neuralized-2 regulates a Notch ligand in cooperation with Mind bomb-1. *J. Biol. Chem.* 281, 36391–36400. [PubMed: 17003037]

- Sturm S, Günther A, Jaber B, Jordan P, Al Kotbi N, Parkar N, Cleary Y, Frances N, Bergauer T, Heinig K, et al. (2019). A phase 1 healthy male volunteer single escalating dose study of the pharmacokinetics and pharmacodynamics of risdiplam (RG7916, RO7034067), a SMN2 splicing modifier. *Br. J. Clin. Pharmacol.* 85, 181–193. [PubMed: 30302786]
- Sumner CJ, Huynh TN, Markowitz JA, Perhac JS, Hill B, Coovert DD, Schussler K, Chen X, Jarecki J, Burghes AH, et al. (2003). Valproic acid increases SMN levels in spinal muscular atrophy patient cells. *Ann. Neurol.* 54, 647–654. [PubMed: 14595654]
- Swoboda KJ, Scott CB, Reyna SP, Prior TW, LaSalle B, Sorenson SL, Wood J, Acsadi G, Crawford TO, Kissel JT, et al. (2009). Phase II open label study of valproic acid in spinal muscular atrophy. *PLoS ONE* 4, e5268. [PubMed: 19440247]
- Swoboda KJ, Scott CB, Crawford TO, Simard LR, Reyna SP, Krosschell KJ, Acsadi G, Elsheik B, Schroth MK, D'Anjou G, et al. ; Project Cure Spinal Muscular Atrophy Investigators Network (2010). SMA CARNI-VAL trial part I: double-blind, randomized, placebo-controlled trial of L-carnitine and valproic acid in spinal muscular atrophy. *PLoS ONE* 5, e12140. [PubMed: 20808854]
- Szklarczyk D, Morris JH, Cook H, Kuhn M, Wyder S, Simonovic M, Santos A, Doncheva NT, Roth A, Bork P, et al. (2017). The STRING database in 2017: quality-controlled protein-protein association networks, made broadly accessible. *Nucleic Acids Res.* 45 (D1), D362–D368. [PubMed: 27924014]
- Van Lint C, Emiliani S, and Verdin E (1996). The expression of a small fraction of cellular genes is changed in response to histone hyperacetylation. *Gene Expr.* 5, 245–253. [PubMed: 8723390]
- Wee CD, Havens MA, Jodelka FM, and Hastings ML (2014). Targeting SR proteins improves SMN expression in spinal muscular atrophy cells. *PLoS ONE* 9, e115205. [PubMed: 25506695]
- Wickramasinghe VO, and Laskey RA (2015). Control of mammalian gene expression by selective mRNA export. *Nat. Rev. Mol. Cell Biol.* 16, 431–442. [PubMed: 26081607]
- Wirth B, Brichta L, Schrank B, Lochmüller H, Blick S, Baasner A, and Heller R (2006). Mildly affected patients with spinal muscular atrophy are partially protected by an increased SMN2 copy number. *Hum. Genet.* 119, 422–428. [PubMed: 16508748]
- Young PJ, DiDonato CJ, Hu D, Kothary R, Androphy EJ, and Lorson CL (2002). SRp30c-dependent stimulation of survival motor neuron (SMN) exon 7 inclusion is facilitated by a direct interaction with hTra2 beta 1. *Hum. Mol. Genet.* 11, 577–587. [PubMed: 11875052]
- Yu HC, Sloan JL, Scharer G, Brebner A, Quintana AM, Achilly NP, Manoli I, Coughlin CR 2nd, Geiger EA, Schneck U, et al. (2013). An X-linked cobalamin disorder caused by mutations in transcriptional coregulator HCFC1. *Am. J. Hum. Genet.* 93, 506–514. [PubMed: 24011988]
- Zhang ML, Lorson CL, Androphy EJ, and Zhou J (2001). An in vivo reporter system for measuring increased inclusion of exon 7 in SMN2 mRNA: potential therapy of SMA. *Gene Ther.* 8, 1532–1538. [PubMed: 11704813]

Highlights

- Genome-wide RNAi screen identifies genes that regulate SMN expression
- Knockdown of RNA processing genes increases SMN through increased nuclear export
- Knockdown of the E3 ligase *Neur12* increases SMN protein levels
- *Neur12* works with *Mib1* to ubiquitinate and promote the degradation of SMN

Author Manuscript

Author Manuscript

Author Manuscript

Author Manuscript

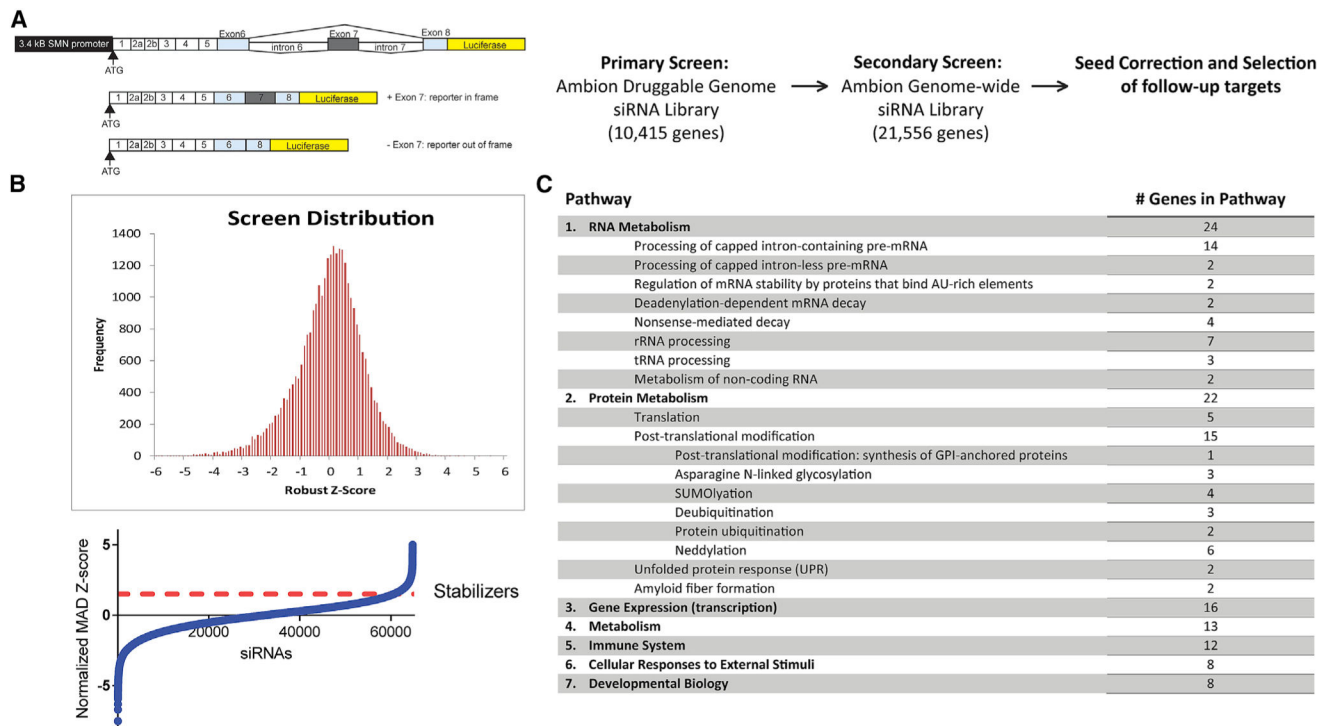


Figure 1. Genome-wide RNAi screen identifies genetic modifiers of SMN expression

(A) Schematic of *SMN2* luciferase reporter cassette stably expressed in HEK293 cells used in an RNAi screen to identify modifiers of SMN. Two independent screens using the Ambion Druggable Genome siRNA library (10,415 genes) and the Ambion Genome-wide siRNA library (21,556 genes) were performed followed by seed correction to eliminate off-target effects.

(B) Distribution of Z scores and distribution of Z scores normalized to median absolute deviation (MAD).

(C) KEGG pathway analysis was used to categorize top hits by predicted molecular function.

See also Figure S1 and Tables S1, S2, and S3.

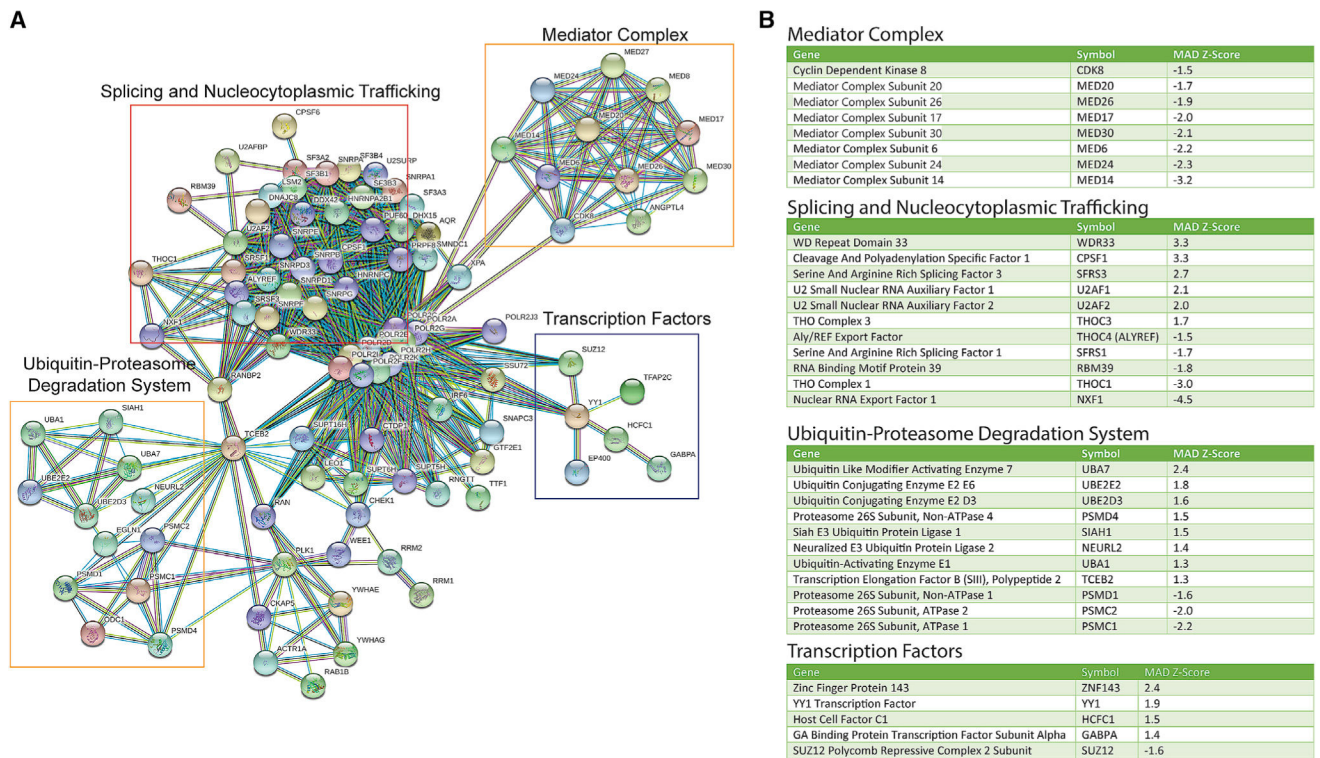


Figure 2. Interactome analysis of top hits
 (A) STRING analysis of top hits showed four gene clusters: mediator complex, splicing and nucleocytoplasmic trafficking, ubiquitin-proteasome degradation system, and transcription factors.
 (B) List of genes and their MAD Z score in each cluster.

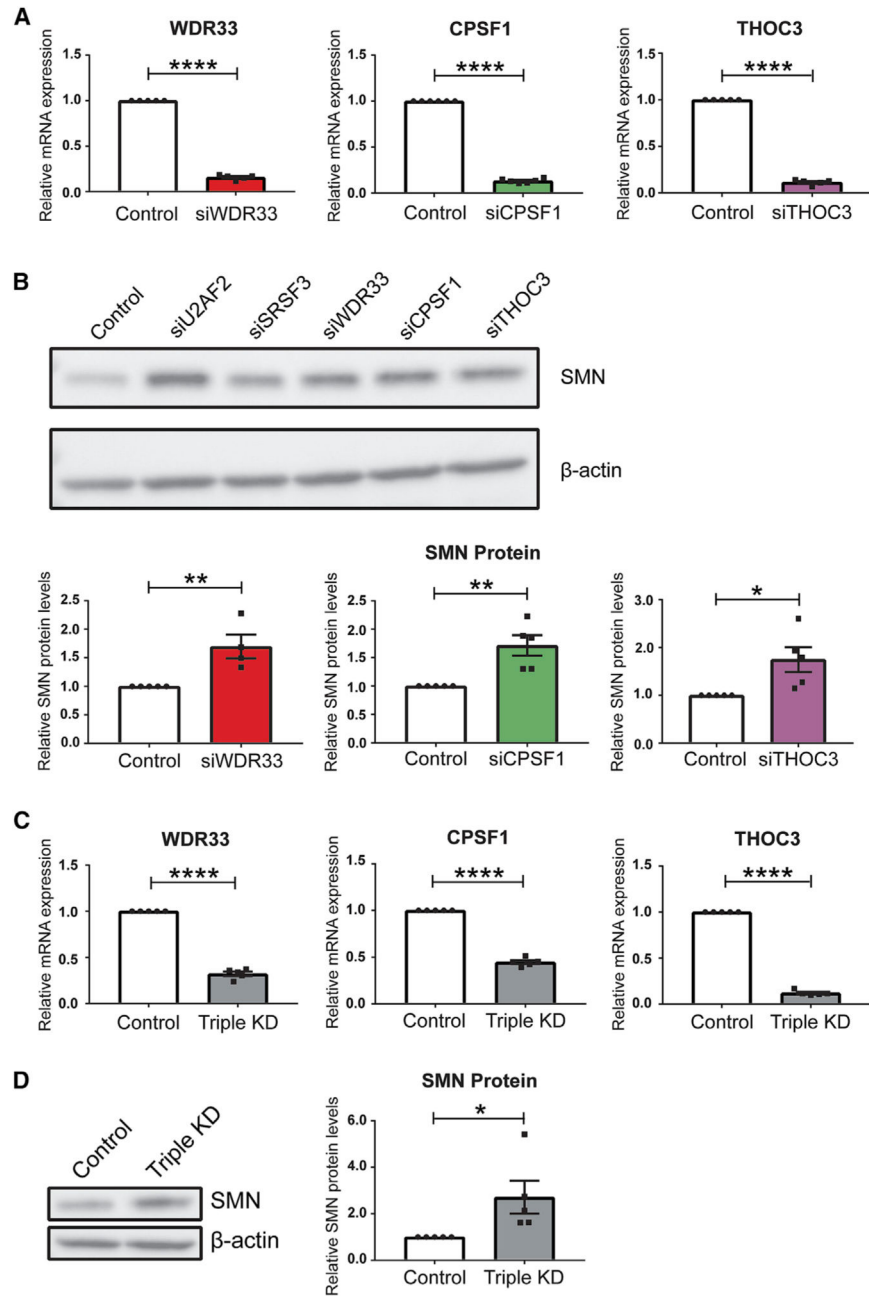


Figure 3. Knockdown (KD) of RNA processing machinery components increases SMN protein levels

SMA patient-derived fibroblasts were transfected with siRNA for 48 h.

(A) Gene expression validates KD of *WDR33*, *CPSF1*, and *THOC3*. Data were analyzed using an unpaired t test (*WDR33* mRNA: $p < 0.0001$; *CPSF1* mRNA: $p < 0.0001$; *THOC3* mRNA: $p < 0.0001$). $n = 5$.

(B) Western blot and quantification of SMN protein levels 48 h after siRNA transfection. SMN protein levels are increased with KD of each gene. Cells transfected with siRNA targeting either *U2AF2* or *SRSF3* were run as a control. Data were analyzed using unpaired

t tests (control versus siWDR33: $p = 0.0064$; control versus siCPSF1: $p = 0.0043$; control versus siTHOC3: $p = 0.0205$). $n = 4-5$.

(C) SMA patient-derived fibroblasts were simultaneously transfected with siRNAs targeting *WDR33*, *CPSF1*, and *THOC3* (triple KD) for 48 h. Gene expression validates KD of *WDR33*, *CPSF1*, and *THOC3*. Data were analyzed using unpaired t tests (*WDR33* mRNA: $p < 0.0001$; *CPSF1* mRNA: $p < 0.0001$; *THOC3* mRNA: $p < 0.0001$). $n = 5$.

(D) Western blot and quantification of SMN protein levels 48 h after transfection with all three siRNAs. SMN protein levels are increased in fibroblasts with all three genes knocked down. Data were analyzed using an unpaired t test ($p = 0.0418$). $n = 5$.

All data are represented as mean \pm SEM. * $p < 0.05$, ** $p < 0.01$, **** $p < 0.0001$. See also Figure S2.

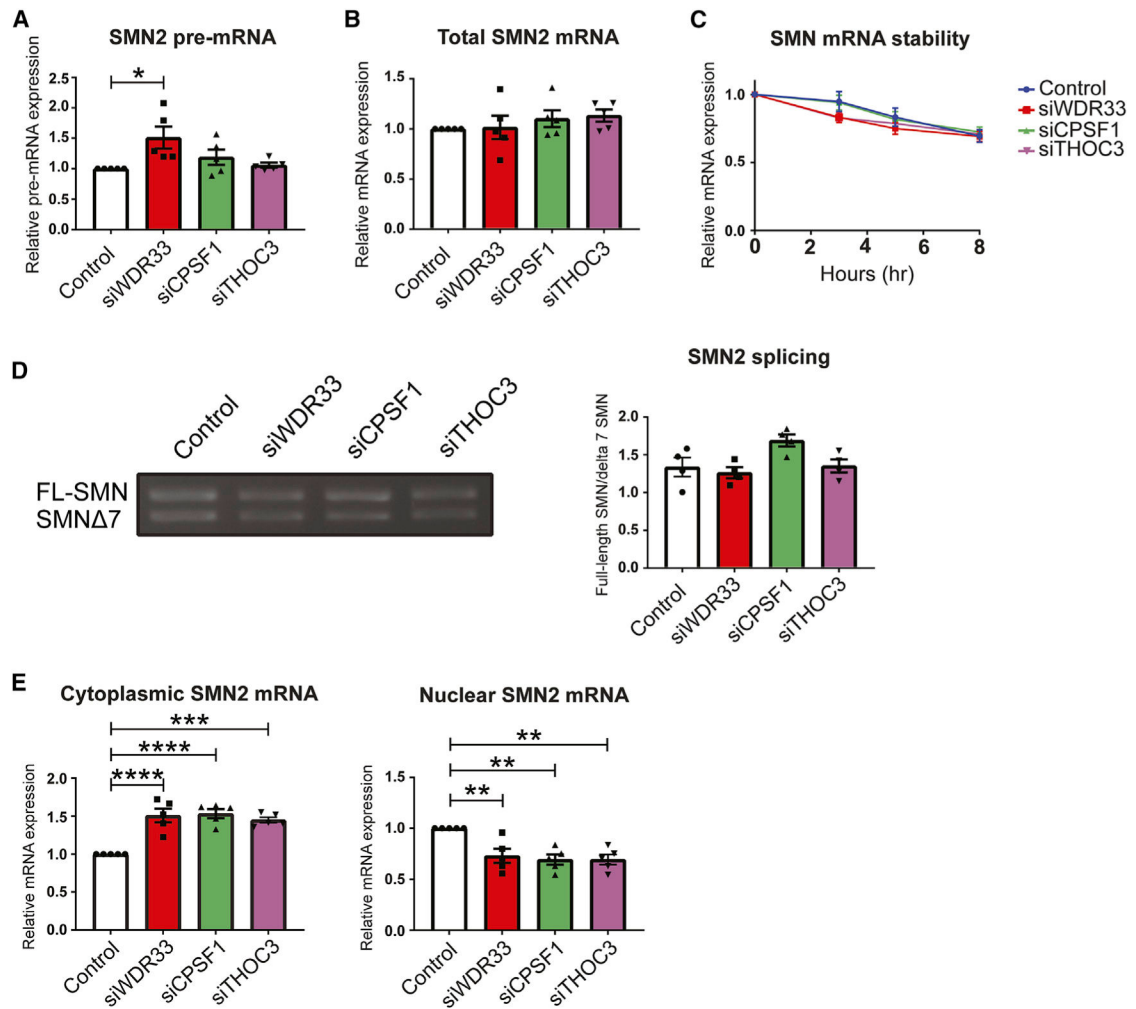


Figure 4. KD of RNA processing machinery components increases cytoplasmic SMN mRNA
SMA patient-derived fibroblasts were transfected with siRNA targeting *WDR33*, *CPSF1*, or *THOC3* for 48 h.

(A and B) SMN2 pre-mRNA (A) and total SMN2 mRNA (B) were examined using qRT-PCR. Total SMN mRNA was unchanged with KD of each gene. SMN pre-mRNA data were analyzed using one-way ANOVA ($F(3,16) = 4.233$, $p = 0.0221$) followed by post hoc Dunnett's multiple comparisons test (control versus siWDR33: $p = 0.0131$; control versus siCPSF1: $p = 0.5059$; control versus siTHOC3: $p = 0.9635$). Total *SMN2* mRNA data were analyzed using one-way ANOVA ($F(3,16) = 0.7025$, $p = 0.5643$). $n = 5$.

(C) SMA patient-derived fibroblasts were transfected with siRNA for 48 h and were then treated with actinomycin D to inhibit transcription. SMN2 mRNA expression was examined for 8 h after the addition of actinomycin D. SMN2 mRNA stability was unchanged with reduction of each gene. $n = 3-4$.

(D) Splicing of the SMN2 transcript and quantification of the ratio of full-length SMN to SMN $\Delta 7$. SMN2 splicing was unchanged with reduction of each gene. *SMN2* splicing data were analyzed using one-way ANOVA ($F(3,12) = 4.071$, $p = 0.0329$) followed by post hoc

Dunnett's multiple comparisons test (control versus siWDR33: $p = 0.8984$; control versus siCPSF1: $p = 0.0537$; control versus siTHOC3: $p = 0.9990$). $n = 5$.

(E) Cytoplasmic and nuclear SMN2 mRNA levels were examined using qRT-PCR. We found the predominantly nuclear MALAT1 mRNA in the nuclear and not the cytoplasmic RNA fractions, confirming the purity of fractionation. Importantly, cytoplasmic SMN mRNA expression was increased with reduction of WDR33, CPSF1, and THOC3. Data were analyzed using one-way ANOVA ($F(3,16) = 19.45$, $p < 0.0001$) followed by post hoc Dunnett's multiple comparisons test (control versus siWDR33: $p < 0.0001$; control versus siCPSF1: $p < 0.0001$; control versus siTHOC3: $p = 0.0001$). $n = 5$. Nuclear SMN mRNA expression was decreased with KD of WDR33, CPSF1, and THOC3. Data were analyzed using one-way ANOVA ($F(3,16) = 8.846$, $p = 0.0011$) followed by post hoc Dunnett's multiple comparisons test (control versus siWDR33: $p = 0.0040$; control versus siCPSF1: $p = 0.0014$; control versus siTHOC3: $p = 0.0014$). $n = 5$.

All data are represented as mean \pm SEM. * $p < 0.05$, ** $p < 0.01$, *** $p < 0.001$, **** $p < 0.0001$. See also Figure S3.

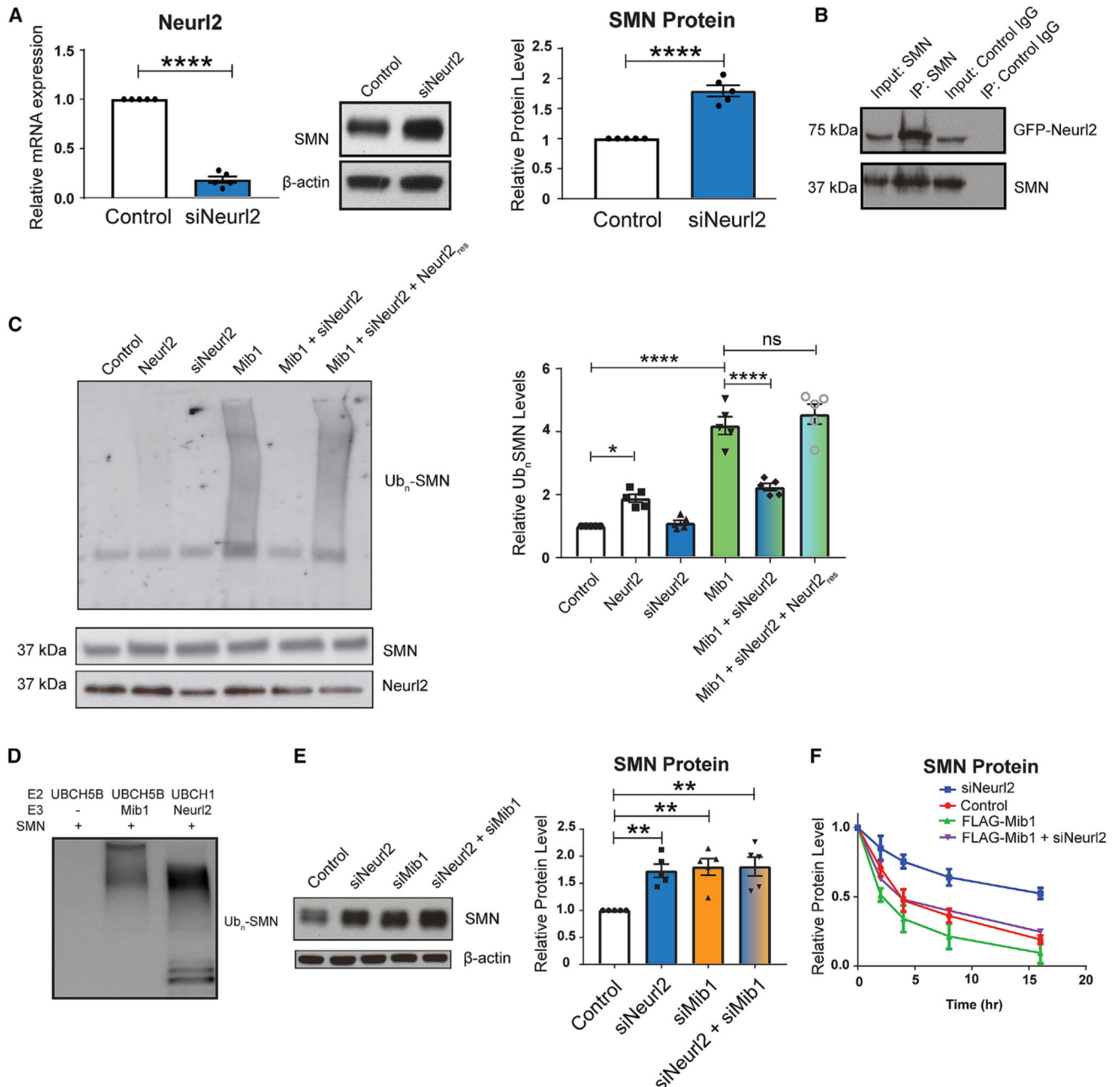


Figure 5. KD of Neur12 blocks SMN degradation to increase SMN protein levels

(A) SMA patient-derived fibroblasts were transfected with siRNA targeting *Neur12*. Gene expression and western blot analysis show that *Neur12* KD resulted in increased SMN levels. Data were analyzed using an unpaired t test (*Neur12* mRNA: $p < 0.0001$; SMN protein: $p < 0.0001$). $n = 5$.

(B) SMA patient fibroblasts were transfected with GFP-*Neur12* or *Neur12*-GFP. SMN was immunoprecipitated, and *Neur12* was associated, confirming their interaction.

(C) Patient fibroblasts were transfected with siRNA targeting *Neur12*, *Mib1*, or both. Western blot analysis of SMN levels 48 h following transfection. Data were analyzed using a one-way ANOVA ($F(5,24) = 65.53$, $p < 0.0001$) followed by post hoc Tukey's multiple

comparisons test (control versus Neurl2: $p = 0.0305$; control versus Mib1: $p < 0.0001$; Mib1 versus Mib1 + siNeurl2: $p < 0.0001$; Mib1 versus Mib1 + siNeurl2 + Neurl2_{res}: $p = 0.7566$). $n = 5$.

(D) Patient cells were transiently transfected with 1 μg HA-ubiquitin and FLAG-Mib1, siRNA targeting Neurl2, or siRNA-resistant Neurl2 (Neurl2_{res}). SMN was immunoprecipitated, and SMN ubiquitination was determined by western blot using an anti-polyubiquitin (FK1) antibody. $n = 3$.

(E) Cell-free SMN ubiquitination assay. Recombinant SMN was incubated with E1 and E2 (UBCH5B or UBCH1) enzymes with or without Mib1 or Neurl2 and ubiquitin for 1 h at 37°C. Western blots were probed with an FK1 antibody. Data were analyzed using one-way ANOVA ($F(3,16) = 8.874$, $p = 0.0011$) followed by post hoc Tukey's multiple comparisons test (control versus siNeurl2: $p = 0.0060$; control versus siMib1: $p = 0.0027$; control versus siNeurl2 + siMib1: $p = 0.0025$; siNeurl2 versus siMib1: $p = 0.9785$; siNeurl2 versus siNeurl2 + siMib1: $p = 0.9740$; siMib1 versus siNeurl2 + siMib1: $p > 0.9999$). $n = 5$.

(F) SMN protein stability following siRNA KD of Neurl2, overexpressing FLAG-Mib1, or both. Data were analyzed using one-way ANOVA (8 h: $F(2,9) = 9.920$, $p = 0.0053$; 16 h: $F(2,9) = 18.93$, $p = 0.0006$) followed by post hoc Tukey's multiple comparisons test (8 h: control versus siNeurl2: $p = 0.0447$; 16 h: control versus siNeurl2: $p = 0.0036$). $n = 4$.

All data are represented as mean \pm SEM. * $p < 0.05$, ** $p < 0.01$, **** $p < 0.0001$.

Table 1.

Clustering of top hits by protein class

Protein class	No. of genes
Nucleic acid binding protein	13
Transporter	7
Cytoskeletal protein	4
Metabolite interconversion enzyme	4
Protein-modifying enzyme	4
Translational protein	4
Gene-specific transcriptional regulator	3
Protein-binding activity modulator	3
Membrane traffic protein	2
Scaffold/adaptor protein	2
Chromatin/chromatin-binding or regulatory protein	1
Defense/immunity protein	1
Intercellular signal molecule	1

The top 100 genes from the RNAi screen were sorted by protein class using a Protein Annotation Through Evolutionary Relationship (PANTHER) analysis.

Author Manuscript

Author Manuscript

Author Manuscript

Author Manuscript

Table 2.

Reidentified modifiers of SMN expression: Genes identified in the RNAi screen that were previously shown to alter SMN expression

Gene symbol	Gene name	Reference
U2AF1	U2 small nuclear RNA auxiliary factor 1	Hastings et al., 2007; Auslander et al., 2020
PUF60	poly-U binding splicing factor 60 kDa	Hastings et al., 2007
HNRNPA2B1	heterogeneous nuclear ribonucleoprotein A2/B1	(Kashima et al., 2007a)
U2AF2	U2 small nuclear RNA auxiliary factor 2	Hastings et al., 2007
UCHL1	ubiquitin carboxyl-terminal esterase L1	Hsu et al., 2010
MIB1	Mindbomb E3 ubiquitin protein ligase 1	Kwon et al., 2013
SRSF11	serine/arginine-rich splicing factor 11	Wee et al., 2014
SRSF3	serine/arginine-rich splicing factor 3	Wee et al., 2014

Author Manuscript

Author Manuscript

Author Manuscript

Author Manuscript

KEY RESOURCES TABLE

REAGENT or RESOURCE	SOURCE	IDENTIFIER
Antibodies		
Mouse anti-SMN	BD Biosciences	Cat# 610647; RRID: AB_397973
Goat anti-mouse IgG, HRP conjugated	Enzo Life Sciences	Cat# BML-SA204-0100; RRID: AB_2051534
Mouse anti- β -actin-peroxidase	Millipore Sigma	Cat# A3854; RRID: AB_262011
Living Colors GFP Polyclonal Antibody	Takara Bio	Cat# 632592; RRID: AB_2336883
Polyubiquitinated conjugates monoclonal (FK1)	Enzo Life Sciences	Cat# BML-PW8805-0500; RRID: AB_2052280
Mouse anti- β -tubulin	Millipore Sigma	Cat# T8453; RRID: AB_1841224
Chemicals, peptides, and recombinant proteins		
Lipofectamine RNAi MAX	Thermo Fisher	Cat# 13778150
Opti-MEM	Thermo Fisher	Cat# 11058021
Luciferin	Promega	Cat# E1601
B-27 supplement	Thermo Fisher	Cat# 17504044
QIAzol Lysis Reagent	QIAGEN	Cat# 79306
iTaq Universal Probes Supermix	Bio-Rad	Cat# 1725134
Actinomycin D	Millipore Sigma	Cat# A9415
Recombinant SMN Protein	Enzo Life Sciences	Cat# ADI-NBP-201-050
Ubiquitin-activating enzyme (UBE1)	Boston Biochem	Cat# E-305
Human recombinant UBCH5B	Enzo Life Sciences	Cat# BML-UW9060-0100
Human recombinant UBCH1	Enzo Life Sciences	Cat# BML-UW9020-0100
Human recombinant Mindbomb-1 Protein	Origene	Cat# TP321377
Human recombinant Neur12 Protein	Abcam	Cat# ab171589
Human recombinant ubiquitin	Enzo Life Sciences	Cat# BML-UW8610-0001
³⁵ S-labeled cysteine-methionine	Perkin Elmer	Cat# NEG072002MC
PCR Supermix	Thermo Fisher	Cat# 10572014
Critical commercial assays		
High Capacity cDNA Reverse Transcriptase Kit	Thermo Fisher	Cat# 4368813
RNeasy Mini Kit	QIAGEN	Cat# 74106
Sure Prep Nuclear or Cytoplasmic RNA Purification Kit	Fisher Scientific	Cat# BP280550
Deposited data		
RNAi screen	This manuscript	PubChem: 1347426
Experimental models: Cell lines		
SMN2-HEK-luciferase reporter cells	Dr. Elliot Androphy, Indiana University (Zhang et al., 2001)	N/A
GM03813 fibroblasts	Coriell	Cat# GM03813; RRID: CVCL_F172

REAGENT or RESOURCE	SOURCE	IDENTIFIER
Oligonucleotides		
See Table S4		N/A
Recombinant DNA		
GFP-Neur12	This manuscript	N/A
Neur12-GFP	This manuscript	N/A
HA-Neur12	This manuscript	N/A
FLAG-Mib1	Dr. Ajay B. Chitnis, NIH (Itoh et al., 2003)	N/A
HA-Neur12 _{res}	This manuscript	N/A
Software and algorithms		
ImageJ	NIH	https://imagej.nih.gov/ij/
GraphPad Prism	Graphpad	https://www.graphpad.com
ImageQuant PhosphorImager	Molecular Dynamics	N/A
Other		
PE ViewLux	Perkin Elmer	https://Perkinelmer.com